



Diffusion behavior of Ni in $Zr_{48}Cu_{36}Ag_8Al_8$ bulk metallic glass within supercooled liquid region

Lin-lin SUN¹, Jun WANG¹, Hong-chao KOU¹, Bin TANG¹, Jin-shan LI¹, Ping-xiang ZHANG^{1,2}

1. State Key laboratory of Solidification Processing, Northwestern Polytechnical University, Xi'an 710072, China;

2. Northwestern Institute for Nonferrous Metal Research, Xi'an 710016, China

Received 8 April 2014; accepted 5 August 2014

Abstract: Diffusion behavior of Ni in $Zr_{48}Cu_{36}Ag_8Al_8$ metallic glass was investigated in the temperature range of 683–723 K by secondary ion mass spectrum (SIMS) and transmission electron microscope (TEM). The diffusivity of Ni in $Zr_{48}Cu_{36}Ag_8Al_8$ is reasonably fitted by a single Arrhenius relation with small effective activation energy. The diffusivity of Ni in $Zr_{48}Cu_{36}Ag_8Al_8$ is an instantaneous function of annealing time in the supercooled liquid region. In addition, a large number of nano-crystals are detected near the interface of Ni– $Zr_{48}Cu_{36}Ag_8Al_8$ diffusion couple, and its width is broader than the Ni diffusion depth determined by SIMS. The results indicate that atomic inter-diffusion is an important factor to promote the formation of nano-crystals within the diffusion zone.

Key words: metallic glasses; diffusion behavior; interface; nano-crystal

1 Introduction

Metallic glasses always transform from metastable state to relaxation or even crystalline state when the atoms receive a certain amount of energy. These transition processes are mainly governed by diffusion, which is important not only from the standpoint of interpreting the glass forming ability, but also for the design of the safe working temperature against crystallization [1,2], such as welding technique [3–5], exterior geometric composite [6] and interior composite [7,8].

For conventional amorphous alloys, the diffusion distances in the permissible temperature–time regime are generally very small with only a few tens of nanometers [9,10], which limited the research on diffusion. Many new bulk metallic glasses with a variety of multi-component alloy systems have been prepared at cooling rates less than 100 K/s [11], which allow the investigation on atomic migration over a wide temperature range including the caloric glass transition, the supercooled state [12–14] and the equilibrium melt [15]. For crystalline metals, solutes in crystals diffuse via single jumps involving vacancies and the

diffusion is determined by the size of the solute. The increasing size dependence shows a typical interstitial- or interstitialcy-type diffusion mechanism, while the decreasing size dependence shows a typical vacancy diffusion mechanism [16]. However, the situation for bulk metallic glasses is much more complex due to its special microstructure. BARTSCH et al [17] reported that the diffusion mechanism occurs by highly collective hopping below a critical temperature (T_C), in accordance with the results from molecular dynamics simulations [18]. Decoupling of the diffusivities of different atomic sizes occurs at around T_C [19]. This implies that the diffusion mechanisms are different when the atomic size varies below this critical temperature. However, a few reports were focused on the interface characteristics of external atomic diffusion to understand the internal microstructure changes of the impurity atoms in metallic glasses. In recent years, Cu–Zr-based BMGs have potential to be a candidate of structure material due to their excellent glass forming ability, high-compressive fracture strength, excellent corrosion resistance and relatively low elements cost [20–22]. In the present work, to analyze diffusion behavior of the smallest atom (Cu) in $Zr_{48}Cu_{36}Ag_8Al_8$ BMG (the maximum diameter of

25 mm), the impurity atom Ni was selected as substitute of Cu in consideration that Ni is adjacent with Cu in the periodic table and the radius difference is very small, besides they are ultimate mutual soluble above 627 K. A Ni/Zr₄₈Cu₃₆Ag₈Al₈ diffusion couple was developed and the diffusion behavior and interface characteristic were investigated by integrating secondary ion mass spectrum (SIMS) and transmission electron microscope (TEM).

2 Experimental

The Zr₄₈Cu₃₆Ag₈Al₈ alloy was prepared by arc melting high purity metals in a Ti-gettered argon atmosphere, and cast into a copper mold to produce BMG rods with 5 mm in diameter. Diffusion couple sample of about 1 mm in thickness was cut with a diamond saw and mechanically polished. Then, the samples were ultrasonically cleaned in acetone. The samples were characterized by DX-2700 X-ray diffractometer using Cu K_α radiation with the continuous scanning mode. Each diffraction analysis shows the typical amorphous pattern without Bragg peaks, as indicated in Fig. 1. The glass transition temperature (*T_g*) and the onset temperature of the first crystallization peak (*T_x*) were determined as 681 and 762 K, respectively by NEZTCH 402 differential scanning calorimeter at a heating rate of 20 K/min. All the samples were sputter-cleaned for about 3 min to avoid diffusion barriers due to the surface oxides under ultra-high vacuum conditions. The Ni layer with 100 nm in thickness was sputter deposited onto the surface. Finally, the specimens were sealed with some small pieces of polished zirconium sheet in an argon-filled quartz capsule. Diffusion annealing was performed in the supercooled liquid region between 683 and 723 K from 300 to 1800 s. Subsequently, samples were quenched into water in order to preserve their amorphous structure. The depth profiles of Ni in Zr₄₈Cu₃₆Ag₈Al₈ bulk metallic glass were

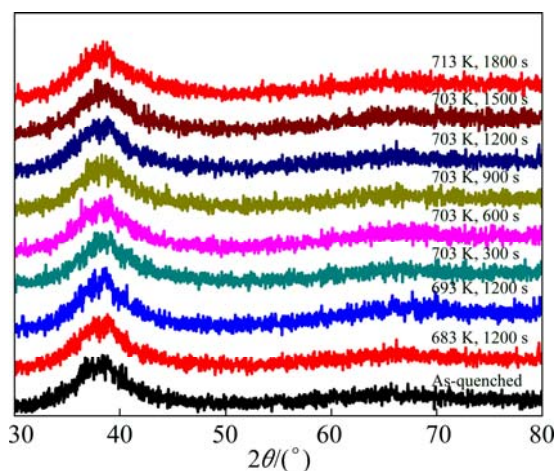


Fig. 1 XRD patterns of Zr₄₈Cu₃₆Ag₈Al₈ metallic glass samples

obtained by ION TOF-SIMS 5 secondary ion mass spectrometry using 5 keV Cs ions for sputter sectioning. The scanned and sputtered area is about 50 μm×50 μm.

The diffusivity was obtained by the thin film solution of the Fick's second law, and the formula is shown as follows [19]:

$$c(x,t) = \frac{I_0}{\sqrt{\pi Dt}} \exp\left(\frac{-x^2}{4Dt}\right) \quad (1)$$

where *D* is the diffusivity, *t* is the annealing time, *x* is the penetration depth, and *I₀* is the initial layer thickness.

The intensity of Ni ions is proportional to the concentration of Ni ions, so the diffusivity is the slope of each straight line ($m = -1/(4Dt)$) which could be obtained by fitting the experimental data according to Eq. (1). The experimental uncertainty of the diffusivity originates from uncertainties in the measurements of depth and temperature [23]. In order to further investigate the interface characteristics of Ni/Zr₄₈Cu₃₆Ag₈Al₈ metallic glass, the microstructure of the diffusion interface was examined by transmission electron microscope (TEM) performed on Tecnai G2F30 with an energy-dispersive spectrometer (EDS).

3 Results and discussion

3.1 Temperature dependence of diffusivity

Figure 2 shows the diffusion profiles of Ni in Zr₄₈Cu₃₆Ag₈Al₈ metallic glass. The diffusivity (*D*) of Ni in Zr₄₈Cu₃₆Ag₈Al₈ metallic glass is calculated from the slope of straight lines. The diffusivity of Ni in Zr₄₈Cu₃₆Ag₈Al₈ metallic glass has an Arrhenius dependence on temperature, as shown in Fig. 3, which can be expressed by $D(T) = 10^{-8.53 \pm 0.12} \exp[-(1.457 \pm 0.162)/(k_B T)]$. It is in accordance with the Arrhenius diagrams reported for other bulk metallic glasses in the supercooled liquid region [12,13]. Compared with Zr-based bulk metallic glasses, the activation energy of

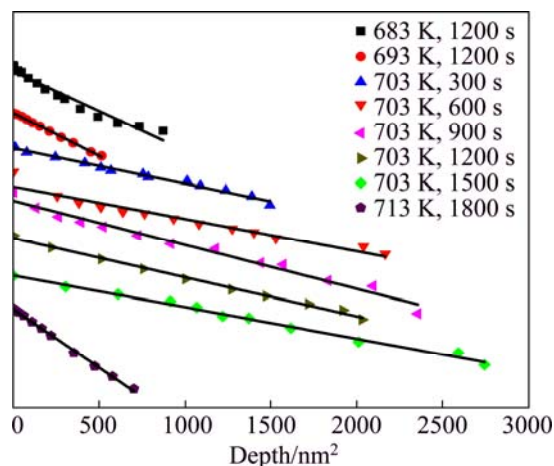


Fig. 2 Concentration-depth profiles of Ni diffusion in Zr₄₈Cu₃₆Ag₈Al₈ metallic glass

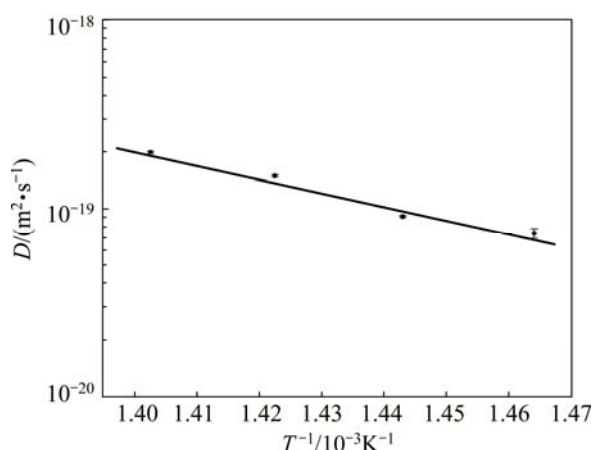


Fig. 3 Arrhenius plot of Ni diffusivities in $Zr_{48}Cu_{36}Ag_8Al_8$ metallic glass (The solid line corresponds to linear Arrhenius fit)

Ni in $Zr_{48}Cu_{36}Ag_8Al_8$ metallic glass is smaller than those of Be in $Zr_{41}Ti_{14}Cu_{12.5}Ni_{10}Be_{22.5}$ and $Zr_{46.75}Ti_{8.25}Cu_{7.5}Ni_{10}Be_{27.5}$. This difference is attributed to the difference of diffusion temperature (the glass transition temperature and the crystallization temperature of $Zr_{41}Ti_{14}Cu_{12.5}Ni_{10}Be_{22.5}$ metallic glass are lower than those of $Zr_{48}Cu_{36}Ag_8Al_8$ metallic glass [24]). Furthermore, structural changes in metallic glass with increasing temperature will affect the Arrhenius parameters [19].

3.2 Diffusion mechanism

It is known that the self-diffusivities of tracer atoms in as-quenched specimens for most of the amorphous alloys decrease with increasing thermal annealing time due to structural relaxations in the glassy state [25]. Moreover, the diffusivity of Ni in the as-quenched $Zr_{48}Cu_{36}Ag_8Al_8$ bulk metallic glass also decreases obviously at first and becomes a constant after certain time within the supercooled liquid region, as shown in Fig. 4. Many studies showed that the decrease of the diffusivity during structural relaxation is related to the transition of diffusion mechanism. It has been proved from single-jump dominated indirect diffusion by vacancy-like defects, to a purely cooperative mechanism via a direct diffusion [26]. Considering that the distribution of free volume is non-uniform within the amorphous alloys, the mechanism of single-atom hopping does not disappear during structural relaxation of a metallic glass. Thus, two distinct processes including the single-atom hopping and highly collective hopping simultaneously contribute to transport in the whole supercooled liquid and the glass state, but their proportion of the two diffusion mechanisms change with annealing time.

Furthermore, it is necessary to classify the diffusion mechanism on the basis of the size of the tracers and the

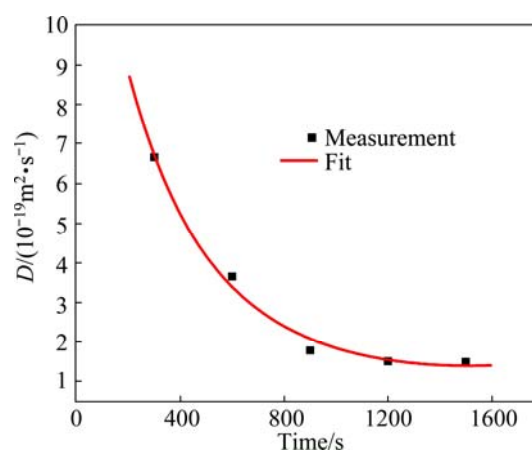


Fig. 4 Instantaneous diffusivities of Ni in metallic glasses as function of annealing time at 703 K

composition of metallic glass according to the diffusion mechanism of the size of solutes in crystals [15]. If the tracer is of the same size or smaller than the smallest component of an alloy, the jumping of diffusive single atom also seems to be possible, like Be in a loosely packed amorphous structure. In the case of large atoms in dense amorphous structures, diffusion requires a cooperative motion involving a cluster of neighboring atoms [27,28].

3.3 Interface characterization

To understand the diffusion behavior of Ni in $Zr_{48}Cu_{36}Ag_8Al_8$ metallic glass, the representative cross-sectional TEM image of Ni/ $Zr_{48}Cu_{36}Ag_8Al_8$ couple after heating at 713 K for 1800 s is shown in Fig. 5. The bright field image (Fig. 5(a)) shows the Ni layer and the obvious diffusion zone in Ni/ $Zr_{48}Cu_{36}Ag_8Al_8$ diffusion couple. The deposited Ni layer with the thickness about 100 nm is in polycrystalline state, as confirmed by

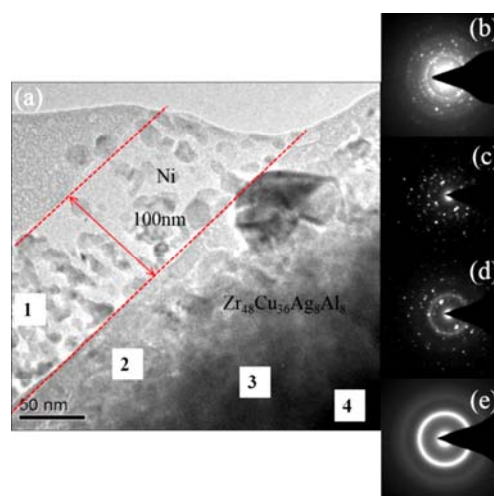


Fig. 5 Bright field TEM image of interface between metallic glass and Ni (a), and diffraction patterns (b, c, d, e) from marked regions 1, 2, 3 and 4 in (a), respectively

selected-area electron diffraction (SAED) pattern in Fig. 5(b). The scattered diffraction patterns distinguished from the amorphous loop shown in Figs. 5(c) and (d) indicate that there exist significant quantities of complex ordered phases near the interface. The structure of the matrix still keeps amorphous, which is confirmed by the SAED pattern in Fig. 5(e). Moreover, a large number of nanoparticles are also clearly observed in the diffusion zone, as shown in Fig. 6. The width of the amorphous–crystal mixture zone is 200–360 nm, which is broader than Ni diffusion depth. Meanwhile, the grains of about 30 nm are detected along the interface by the dark field image. The precipitated phases in the diffusion zone characterized by the corresponding EDS are rich in Cu, Zr and small amounts of Ni, as listed in Table 1. It is detected as Zr_2Cu according to the results of EDS and TEM. Accordingly, the composition of white particles denoted as “E” near the metallic glass is detected.

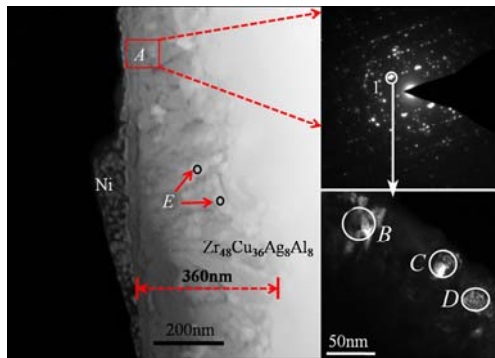


Fig. 6 TEM image of interface between $Zr_{48}Cu_{36}Ag_8Al_8$ metallic glass and Ni annealed at 713 K

Table 1 EDS analysis results of diffusion zone in Fig. 6

Position	Mole fraction/%				
	Ni	Cu	Zr	Ag	Al
B	0.52	23.74	53.33	13.57	8.84
C	1.47	13.14	67.66	–	17.73
D	0.73	38.15	55.32	5.80	–
E	–	11.82	77.08	–	11.10

A simplistic schematic of the interface crystallization growth path can be established as shown in Fig. 7. From Fig. 7, it can be seen that the original interface grows into both Ni layer and $Zr_{48}Cu_{36}Ag_8Al_8$ metallic glass simultaneously. Due to the higher quasi-vacancy near the interface, the diffusion rate of atoms is higher than that in the $Zr_{48}Cu_{36}Ag_8Al_8$ metallic glass. This is the main reason for the formation of nano-crystals (about 30 nm) along the interface. In previous experiment, we found that a number of nano-particles occurred within the diffusion zone of Zr-based BMG/copper laminated composite [24]. These

results suggest that the atomic inter-diffusion is an important factor to promote the formation of nano-particles within the diffusion zone.

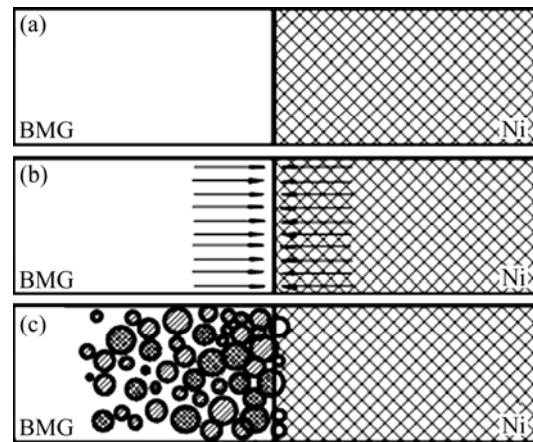


Fig. 7 Schematic of interface crystallization path at 713 K: (a) Before diffusion; (b) Atom inter-diffusion between BMG and Ni; (c) Nano-crystal formation after 1800 s (Different circles represent different components of nano-crystals, respectively)

Small variations in chemical composition or further elements addition will change the stability of the glass and form different metastable phases or even crystalline phase during annealing [29,30]. In addition, there exists a driving force for metastable system of metallic glasses to relaxation and crystallization during heat treatment above the glass transition, which also leads to the formation of crystalline phase. Based on the above analysis, the amorphous–crystal mixture zone probably depends on the twofold reasons: one can be explained by mutual diffusion of the atoms between Ni layer and $Zr_{48}Cu_{36}Ag_8Al_8$ metallic glass, and the other is prompted by composition fluctuation due to the atomic inter-diffusion between Ni and $Zr_{48}Cu_{36}Ag_8Al_8$ metallic glass. Whether or not the formation of nano-crystals near the interface will influence the atom diffusion mechanism of amorphous alloy needs further research.

4 Conclusions

1) The diffusivities of Ni atoms in $Zr_{48}Cu_{36}Ag_8Al_8$ metallic glasses were fitted by a single Arrhenius relation with $D(T)=10^{-8.53\pm 0.12}\exp[(-1.457\pm 0.162)/(k_B T)]$. The small effective activation energy is attributed to the different diffusion temperature and structural changes.

2) The width of the amorphous–crystal mixture zone (200–360 nm) near the interface is broader than Ni diffusion depth, which is attributed to the consequences of the interaction of the inter-diffusion reaction from Ni/ $Zr_{48}Cu_{36}Ag_8Al_8$ and composition fluctuation near the amorphous matrix.

References

- [1] SCHROERS J. Processing of bulk metallic glass [J]. *Advanced Materials*, 2010, 22: 1566–1597.
- [2] BØTTIGER J, CHECHENIN N G, KARPE N, KROG J P. Diffusion in thin-film amorphous metallic alloys[J]. *Nucl Instr and Meth in Phys Res B*, 1994, 85: 206–215.
- [3] KIM J, KAWAMURA Y. Electron beam welding of the dissimilar Zr-based bulk metallic glass and Ti metal [J]. *Scripta Mater*, 2007, 56: 709–712.
- [4] OHKUBO T, SHOJI S, KAWAMURA Y, HONO K, GRIESCHE A, MACHT M P, FROHBERG G. Nanostructure analysis of friction welded Pd–Ni–P/Pd–Cu–Ni–P metallic glass interface [J]. *Scripta Mater*, 2005, 53: 493–497.
- [5] MA GUO-FENG, ZHANG Bo, ZHANG Hai-feng, HU Zhuang-qi. Growth kinetics for intermetallic compound layer between molten In–Sn alloy and CuZr-based bulk metallic glass [J]. *Transactions of Nonferrous Metals Society of China*, 2012, 22(4): 837–841.
- [6] RAGANI J, VOLLAND A, GRAVIER S, BLANDIN J J, SUÉRY M. Metallic glass/light alloy (MEGA) multimaterials elaborated by co-pressing at high temperature [J]. *J Alloys Comps*, 2010, 495: 323–326.
- [7] QIN C L, ZHANG W, ASAMI K, KIMURA H, WANG X M, INOUE A. A novel Cu-based BMG composite with high corrosion resistance and excellent mechanical properties [J]. *Acta Mater*, 2006, 54: 3713–3719.
- [8] WANG K, FUJITA T, PAN D, NIEH T G, INOUE A, KIM D H, CHEN M W. Interface structure and properties of a brass-reinforced Ni₅₉Zr₂₀Ti₁₆Si₂Sn₃ bulk metallic glass composite [J]. *Acta Mater*, 2008, 56: 3077–3087.
- [9] ALPAS A T, EMBURY J D. Flow localization in thin layers of amorphous alloys in laminated composite structures [J]. *Scripta Mater*, 1988, 22: 265–270.
- [10] TYAGI A K, MACHT M P, NAUNDORF V. Self diffusion measurements of nickel in Fe₄₀Ni₃₈Mo₄B₁₈ glass by secondary ion mass spectrometry [J]. *Scripta Mater*, 1990, 24: 2369–2374.
- [11] PETER A, JOHNSON W L. A highly processable metallic glass: Zr_{41.2}Ti_{13.8}Cu_{12.5}Ni_{10.0}Be_{22.5} [J]. *Appl Phys Lett*, 1993, 63: 2342–2344.
- [12] KNORR K, MACHT M P, FREITAG K, MEHRER H. Self-diffusion in the amorphous and supercooled liquid state of the bulk metallic glass Zr_{46.75}Ti_{8.25}Cu_{7.5}Ni₁₀Be_{27.5} [J]. *J Non-Cryst Sol*, 1999, 250–252: 669–673.
- [13] FIELITZ P, MACHT M P, NAUNDORF V, FROHBERG G. Diffusion in ZrTiCuNiBe bulk glasses at temperatures around the glass transition [J]. *J Non-Cryst Sol*, 1999, 250–252: 674–678.
- [14] EHMLER H, RÄTZKE K, FAUPEL F. Isotope effect of diffusion in the supercooled liquid state of bulk metallic glasses [J]. *J Non-Cryst Sol*, 1999, 250–252: 684–688.
- [15] GRIESCHE A, MACHT M P, SUZUKI S, KRAATZ K H, FROHBERG G. Self-diffusion of Pd, Cu and Ni in Pd-based equilibrium melts [J]. *Scripta Mater*, 2007, 57: 477–480.
- [16] FAUPEL F, FRANK W, MACHT M P, MEHRER H, NAUNDORF V, RÄTZKE K, SCHÖBER H R, SHARMA S K, TEICHLER H. Diffusion in metallic glasses and supercooled melts [J]. *Rev Mod Phys*, 2003, 75: 237–280.
- [17] BARTSCH A, ZÖLLMER V, RÄTZKE K, MEYER A, FAUPEL F. Diffusion and viscous flow in bulk glass forming alloy [J]. *J Alloys Comps*, 2011, 509: S2–S7.
- [18] ZHU A, SHIFLET G J, POON S J. Diffusion in metallic glasses: Analysis from the atomic bond defect perspective [J]. *Acta Mater*, 2008, 56: 3550–3557.
- [19] RÄTZKE K, ZÖLLMER V, BARTSCH A, MEYER A, FAUPEL F. Diffusion in bulk-metallic glass-forming Pd–Cu–Ni–P alloys: From the glass to the equilibrium melt [J]. *J Non-Cryst Sol*, 2007, 353: 3285–3289.
- [20] CHIANG C L, CHU J P, LO C T, NIEH T G, WANG Z X, WANG W H. Homogeneous plastic deformation in a Cu-based bulk amorphous alloy [J]. *Intermetallics*, 2004, 12: 1057–1061.
- [21] ZHANG W, ZHANG Q, QIN C, INOUE A. Synthesis and properties of Cu–Zr–Ag–Al glassy alloys with high glass-forming ability [J]. *Mater Sci Eng B*, 2008, 148: 92–96.
- [22] PI Jin-hong, PAN Ye, WU Ji-li, ZHANG Lu, HE Xian-cong. Preparation and properties of novel Cu-based bulk metallic glasses Cu_{55-x}Zr₃₇Ti₈In_x [J]. *Transactions of Nonferrous Metals Society of China*, 2013, 23(10): 2989–2993.
- [23] EHMLER H, HESEMANN A, RÄTZKE K, FAUPEL F, GEYER U. Mass dependence of diffusion in a supercooled metallic melt [J]. *Phys Rev Lett*, 1998, 80: 4919–4922.
- [24] SUN L L, WANG J, KOU H C, TANG B, LI J S, ZHANG P X. Interface characteristics of a Zr-based BMG/copper laminated composite [J]. *Surf Interface Anal*, 2013, 46(2): 61–64.
- [25] HORVÁTH J, PFAHLER K, ULFERT W, FRANK W, KRONMÜLLER H. Diffusion in amorphous metallic alloys [J]. *Mater Sci Forum*, 1987, 15–18: 523–528.
- [26] RÄTZKE K, HÜPPE P W, FAUPEL F. Transition from single-jump type to highly cooperative diffusion during structural relaxation of a metallic glass [J]. *Phys Rev Lett*, 1992, 68: 2347–2349.
- [27] FRANK W, HÖRNER A, SCHARWAECHTER P, KRONMÜLLER H. Diffusion in amorphous metallic alloys [J]. *Mater Sci Eng A*, 1994, 179–180: 36–40.
- [28] GEYER U, SCHNEIDER S, JOHNSON W L, QIU Y, TOMBRELLO T A, MACHT M P. Atomic diffusion in the supercooled liquid and glassy states of the Zr_{41.2}Ti_{13.8}Cu_{12.5}Ni₁₀Be_{22.5} alloy [J]. *Phys Rev Lett*, 1995, 75: 2364–2367.
- [29] KELTON K F. Liquid structure and long range diffusion: Their impact on glass formation and nanoscale devitrification [J]. *Intermetallics*, 2006, 14: 966–971.
- [30] LIU L, ZHAO X, MA C, ZHANG T. Kinetics of crystallization process for Pd-based bulk metallic glasses [J]. *Intermetallics*, 2009, 17: 241–245.

Ni 在过冷液态 Zr₄₈Cu₃₆Ag₈Al₈ 非晶合金中的扩散行为

孙琳琳¹, 王军¹, 寇宏超¹, 唐斌¹, 李金山¹, 张平祥^{1,2}

1. 西北工业大学 凝固技术国家重点实验室, 西安 710072; 2. 西北有色金属研究院, 西安 710016

摘要: 采用二次离子质谱(SIMS)以及透射电镜(TEM)研究在 683~723 K 温度范围内 Ni 原子在 Zr₄₈Cu₃₆Ag₈Al₈ 非晶合金中的扩散行为。在过冷液相区内, Ni 原子在 Zr₄₈Cu₃₆Ag₈Al₈ 非晶合金中的扩散系数满足单一的 Arrhenius 关系式, 具有较低的激活能, 在过冷液相区内其扩展数系数是一个随退火时间变化的函数。此外, 在界面附近有大量的纳米晶形成, 其宽度大于通过二次离子质谱检测到的 Ni 原子扩散深度。结果表明: 原子互扩散是促使界面纳米晶形成的重要因素。

关键词: 非晶合金; 扩散行为; 界面; 纳米晶

(Edited by Xiang-qun LI)